Fracture Mechanics of Concrete Structures
Proceedings FRAMCOS-3
AEDIFICATIO Publishers, D-79104 Freiburg, Germany

EXPERIMENTAL INVESTIGATION INTO THE SIZE DEPENDENCE OF FRACTURE MECHANICS PARAMETERS

B. Trunk, and F.H. Wittmann,
Laboratory for Building Materials,
Swiss Federal Institute of Technology Zürich, Switzerland

Abstract
Specific fracture energy and strain softening have proved to be material parameters, which describe the cracking of cementitious materials in a realistic way. But these parameters depend on specimen size and geometry as strength does. In order to investigate the influence of specimen size on the fracture mechanics parameters wedge splitting tests have been carried out on geometrically similar specimens with a size of the characteristic specimen dimension ranging between 50 and 3200 mm. Specimens prepared with hardened cement paste, mortar, normal concrete and dam concrete have been tested. The influence of the maximum grain size on the size dependence of the fracture mechanics parameters has been studied. The size of the maximum aggregate was varied in the range between 0 mm (hardened cement paste) and 125 mm (dam concrete). Experimental results obtained by means of the wedge splitting test are compared with results determined by direct tension tests. It is shown that fracture energy increases with size until it reaches a constant value. Tensile strength of concrete decreases instead. Fracture energy increases strongly with increasing aggregate size.
Key words: Experimental investigation, fracture energy, strain softening, influence of aggregate size, influence of specimen size

1 Introduction

In laboratory tests, fracture mechanics parameters are often obtained on relatively small specimens compared to the size of a real structure. From many fracture mechanics tests it is known, that these parameters depend on both specimen size and geometry. This effect has been observed before by many authors as for example Brühwiler (1989), Wittmann (1990), Slowik et al. (1992). But in most models of fracture mechanics it is assumed that these parameters are material constants and independent of size and geometry.

In investigating the size dependence of fracture mechanics parameters we have to distinguish at least three size ranges. If the size of a structural element is comparatively small with respect to the maximum heterogeneity of the material we have to take the heterogeneity of the material's structure into consideration. In concrete technology the maximum aggregate size is generally assumed to be the largest element of heterogeneity. In this size range all models based on continuum mechanics can not be applied. In order to study the influence of the heterogeneity on the global behaviour of a bulk material, Roelfstra et al. (1985) introduced the concept of numerical concrete. For specimens, in which the heterogeneity of the material is comparatively small with respect to the smallest specimen dimension, and the non-linear behaviour of the bulk material in front of the crack tip at high strains is comparatively large with respect to the initial crack length non-linear damage models like the fictitious crack model as proposed by Hillerborg et al. (1976) can be used. For very large structures at least, in which the inelastic fracture process zone (FPZ) in front of the crack tip is small compared to the initial crack length the structural behaviour becomes more brittle. Models derived from linear-elastic fracture mechanics (LEFM) like R-curve modelling or in extreme cases LEFM may be used.

For cement based materials the size of the non-linear deformation zone in front of the crack tip (fracture process zone) and the specific fracture energy G_f depend strongly on the maximum aggregate size Φ_{max}. This has to be taken into consideration in any attempt of scaling.

2 Experimental procedure

2.1 Test series and preparation of specimens

Hardened cement paste (HCP), two fine grained mortars (FM I, FM II), two standard mortars (M I, M II), a normal concrete (NC) and three different types of dam concrete (DC I, DC II, DC III) have been tested. The relevant mix data of each material are summarized in Table 1.

Table 1. Composition and range of size of the different materials tested

Material	Water/Cement Ratio	Cement Content c [kg/m^3]	Max. Aggregate Size Φ_{max} [mm]	Specimen Size Range H [mm]
HCP(0.75)	0.32	2100	-	100-400
HCP(0.5)	0.32	2100	-	100-800
FM I	0.35	1000	Filler (60 % 0-4 mm)	50-800
FM II	0.5	625	0.7	50-800
M I	0.48	450	0.4	50-800
M II	0.55	450	0.4	50-800
NC	0.5	300	32	50-3200
DC I	0.5	250	63	200-800
DC II	0.66	175	125	200-1600
DC III	0.47	250	125	200-3200

The concrete specimens with the exception of the dam concrete DC I were stored for more than one year under sealed conditions in order to obtain parameters which are characteristic for existing structures and to avoid any influence of age during testing. The specimens made of dam concrete DC I were stored for 3 months before testing. All mortar specimens were stored between 90 and 120 days at 70 % relative humidity at 20 °C. The specimens made of hardened cement paste were stored at 100 % relative humidity at 20 °C to avoid crack formation by drying shrinkage.

Some halfs of the wedge splitting specimens formed during testing were cut with a diamond saw into smaller elements and tested again. For all the wedge splitting specimens expect the specimens with a height H of 50 mm the specimen height H is equal to the width. For technical reasons the specimens with a height of 50 mm were 100 mm wide. The ratio between the initial notch length a_0 to the height H was 0.75 for the series HPC(0.75) and for all others 0.5. The size range for each test series is given in table 1. The characteristic specimen dimensions H have always been doubled from one size up to the next bigger one within the given size range.

2.2 Testing procedure

2.2.1 Wedge splitting test

A schematical illustration of the test set-up is given in Fig. 1. Two wedges are pressed symmetrically between four roller bearings in order to split the specimen into two halves. The test set up is similar to the RILEM recommendation AAC 13.1 (1994) with one difference, however, that the specimen is placed on two line supports and not only on one single line support in the centre of the specimen. The supports are right under the mass concentration points of each half specimen. The main advantage of this loading arrangement is that for large specimens the influence of the dead weight of each half specimen on the experimental results is minimized. A similar experimental arrangement has also been used by Guofan et al. (1991) and van Gils et al. (1995).

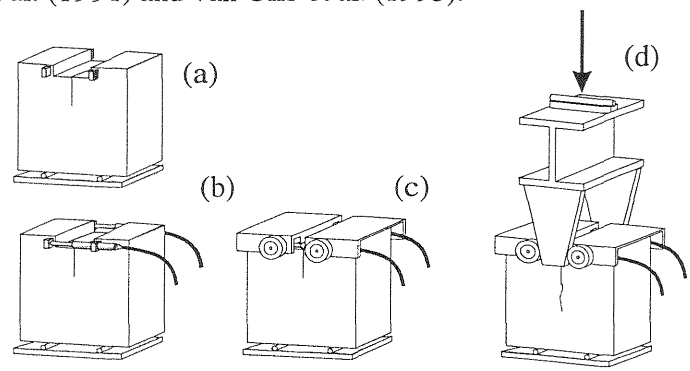

Fig. 1. Schematic representation of the wedge splitting test: (a) specimen on 2 linear supports, (b) displacement transducers on both sides of the specimen, (c) steel loading devices with roller bearings, (d) traverse with wedges

The crack mouth opening displacement (CMOD) at both sides of the specimen at the level of the loading points, (see Fig. 1) and the applied vertical load F are measured. From the measured vertical load and the known wedge angle the horizontal splitting force is calculated. The measured CMOD is the mean value of the two displacement transducers on the two opposite sides of the specimen. All tests were run under CMOD control. For large specimens two additional displacement transducers for the displacement control were placed on both sides of the specimen at half height of the notch to stabilise the experiment.

The work of fracture is calculated from the area under the splitting force CMOD diagram. The specific fracture energy G_f is the work of fracture divided by the ligament area A_L.

In order to determine numerically the non-linear fracture mechanics parameters from all experimental results of one series a mean load deflection diagram has been calculated first. By means of an inverse analysis based on finite element calculations as described by Roelfsta et al. (1986) the strain softening diagram approximated by a bilinear function is obtained. The non-linear finite element program SOFTFIT initially implemented by Roelfstra (1986) is used. In Fig. 2 an example of a bilinear approximated strain softening diagram with all significant parameters is given. The specific fracture energy G_f is equal to the area under the strain softening curve.

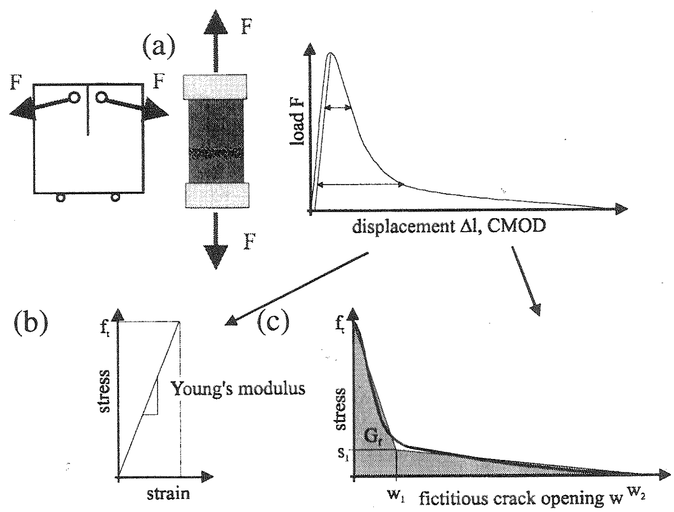

Fig. 2. Parameters of the strain softening relation as approximated by a bilinear function: (a) force-displacement-curve as a test result; (b) linear elastic material behaviour, before the tensile strength is reached and later outside the FPZ; (c) strain-softening-relation with a bilinear approximation

2.2.2 Direct tension test

In a uniaxial direct tensile test cylindrical specimens have been loaded. To achieve a nearly homogeneous uniaxial stress distribution all over the specimen geometry it is necessary to avoid stress concentrations at the loading interface. In addition the attachments to the loading machine have to be restrained against rotation. Otherwise the post peak path of the load deflection curve bifurcates (Bažant et al. (1993)). However, due to the relative brittleness of concrete a very stiff and closed loop controlled testing machine has to be used for determining the strain softening behaviour directly (Petersson (1981)).

To meet these requirements the test specimens were glued to aluminium cylinders with approximately the same lateral contraction of the endfaces to avoid shear stresses and a triaxial state of stress. Both, the specimen and the aluminium cylinders, have the same diameter. The aluminium cylinders were screwed on steel supporting plates for rotational stiff attachment to the testing machine.

Fig. 3 shows the experimental set-up for the direct tensile tests. Steel bars were attached parallel to the specimen in order to increase the stiffness of the machine. The tests were run under displacement controlled conditions using a servo-hydraulic testing machine with a maximum force of 1'600 [kN].

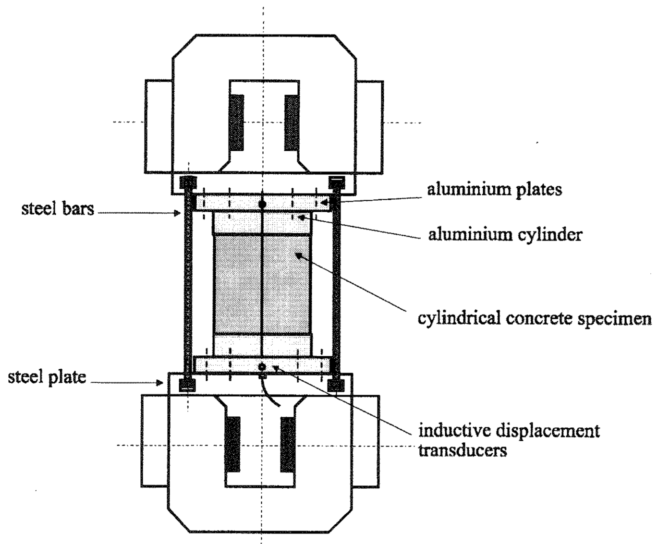

Fig. 3. Experimental set-up for direct tension tests with a servo-hydraulic testing machine

3 Experimental results

3.1 Observed behaviour

In Fig. 4 first of all, all measured force-CMOD-diagrams for the size H = 200 mm of normal concrete specimens are shown. The mean curve obtained from these experimental results is also shown in Fig.4.

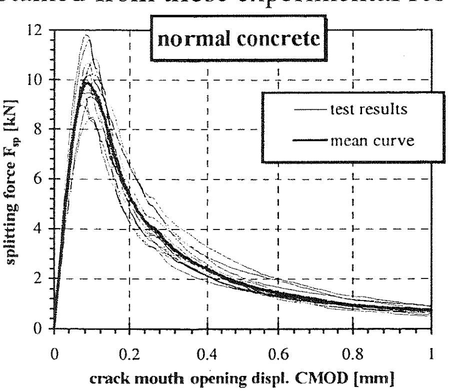

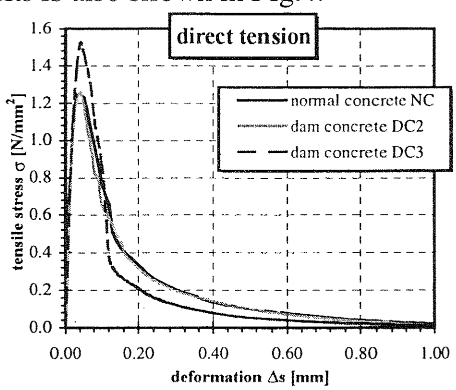

Fig. 4. Determined mean curve from all test results (H = 200 mm)

Fig.5. Mean load elongation curves from all direct tension tests

In Fig. 6 the mean load deformation curves for the normal concrete for each specimen size are given as an example. From the descending branch it can already be seen, that the brittleness of the tested specimens increases with the specimen size. The mean stress displacement curves from the direct tension tests for the normal concrete and the two types of dam concrete DC II and DC III are given in Fig. 5.

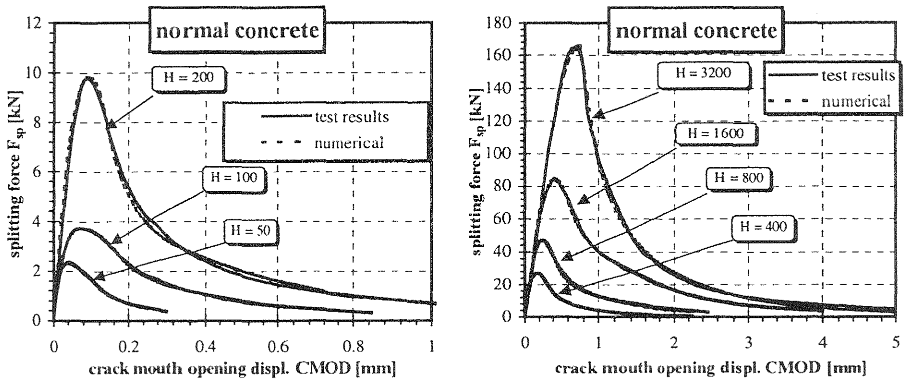

Fig. 6. Mean load deformation curves and numerical simulations for all normal concrete specimens

3.2 Fracture energy

From the directly observed behaviour as shown for example in Fig. 5 and Fig. 6 fracture energy and strain softening have been determined.

In Fig. 7 and 8 the dependence of the specific fracture energy G_f is given as function of the ligament length H_L. As it can be seen that the specific fracture energy G_f increases considerably with the specimen size.

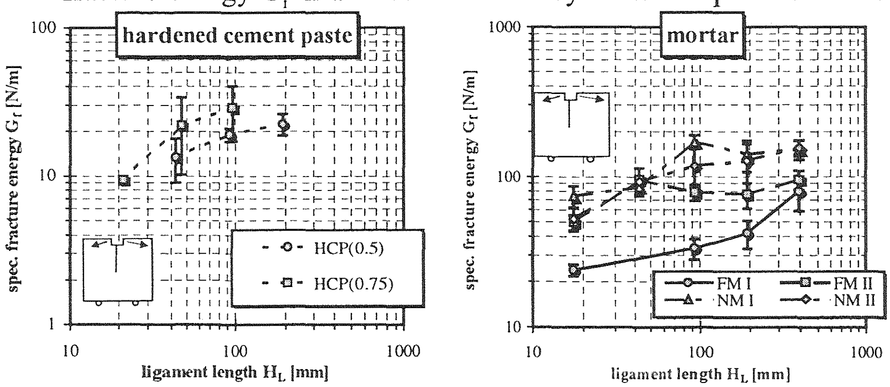

Fig. 7. Specific fracture energy as function of ligament length for hardened cement paste and all types of mortar

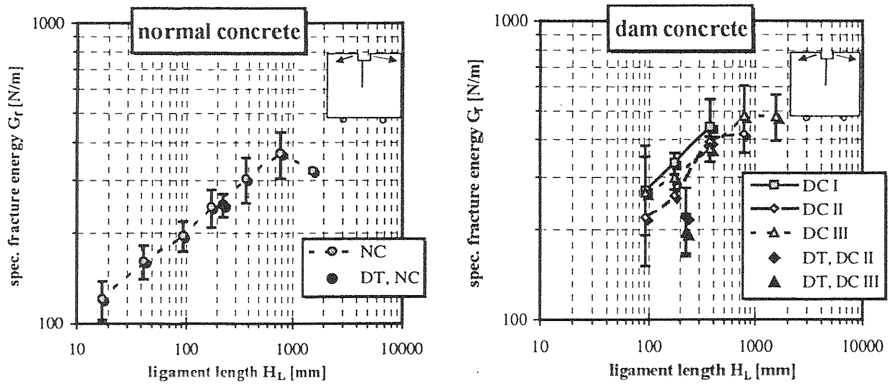

Fig. 8. Specific fracture energy as function of ligament length for normal and all types of dam concrete

Some of the HCP specimens and all with a height of 800 mm as well as some fine grained mortar specimens failed in a brittle way. For this reason it was not possible to determine fracture energy for these specimens. As it can be seen from the series FM II, NM I, NM II, NC, DC II and DC III the fracture energy increases with increasing specimen size, until a limit value seems to be reached (see Trunk et al. (1998)). For the dam concrete DC I the size range covered apparently was too small and therefore no limit value has been reached. In Fig. 8 values of the specific fracture energy as determined by means of the direct tension test (DT) are also given. In this case an effective ligament length H_L has been calculated such as to obtain a ligament area equal to the cross section of the cylinders tested in direct tension. For normal concrete it can be seen, that the value of fracture energy G_f as determined by means of direct tension tests agrees well with the results obtained by the wedge splitting tests. While the fracture energy for the two types of dam concrete DC II and DC III determined by means of the direct tension test is lower than the fracture energy determined from wedge splitting tests. It must be noted in this context that for dam concrete the diameter of the direct tension cylinders was only about 2.7-times the max. aggregate size and therefore the representative volume was hardly reached.

4 Evaluation of results

In Fig. 9 the dependence of the specific fracture energy G_f is given as function of the maximum aggregate size Φ_{max}. The maximum aggregate size of the cement paste is assumed to be equal to the average particle size of the Portland cement, i.e. 10 μm. As may have been expected the specific fracture energy G_f increases with maximum aggregate size. This also means that the ductility of the material increases with maximum aggregate size Φ_{max}.

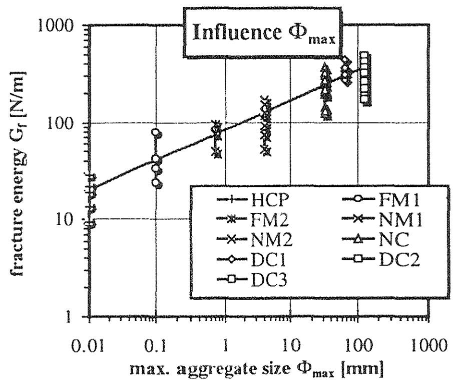

Fig. 9. Specific fracture energy as function of maximum aggregate size

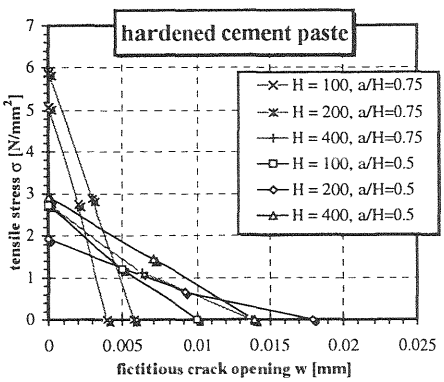

Fig. 10. Strain softening diagrams for hardened cement paste

The relationship in Fig. 9 can be represented approximately by a power function:

$$G_f = a \cdot \Phi_{max}{}^{n} \tag{1}$$

with a = 83.4 and n = 0.31.

The bilinear approximated strain softening diagram has been calculated from the measured load deflection curves as described above. The calculated strain softening curves are given in Fig. 10 to 14 for each material type and specimen size.

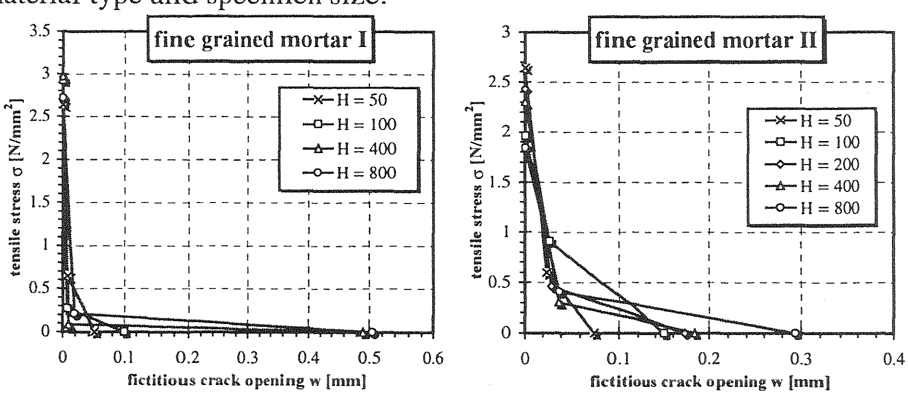

Fig. 11. Strain softening diagrams for the two types of fine grained mortar

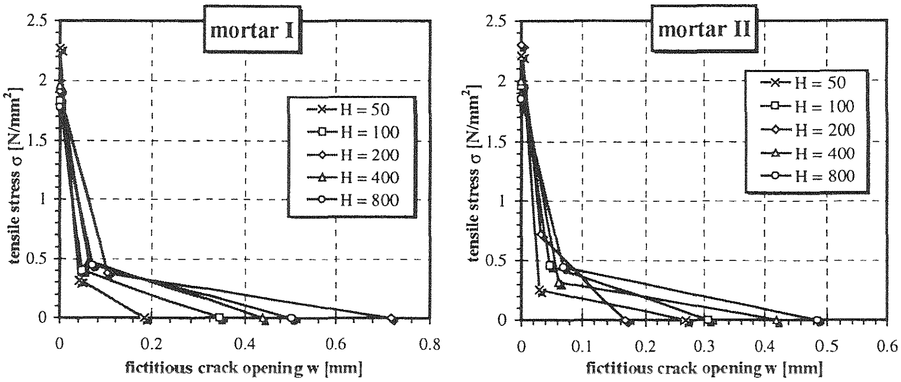

Fig. 12. Strain softening diagrams for the two types of normal mortar

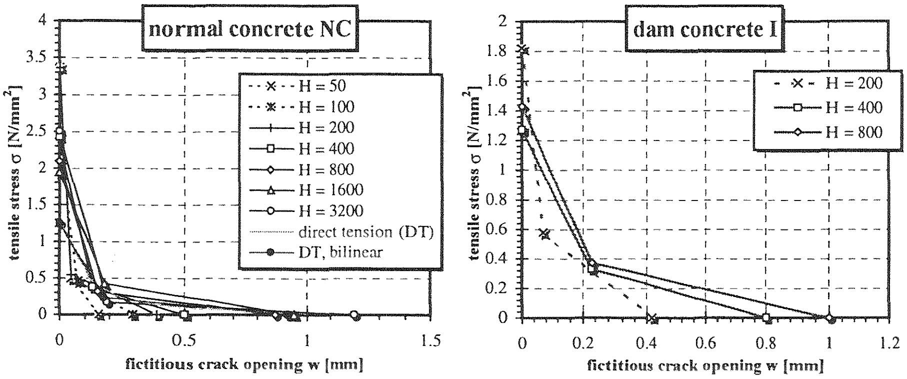

Fig. 13. Strain softening diagrams for normal concrete and dam concrete I

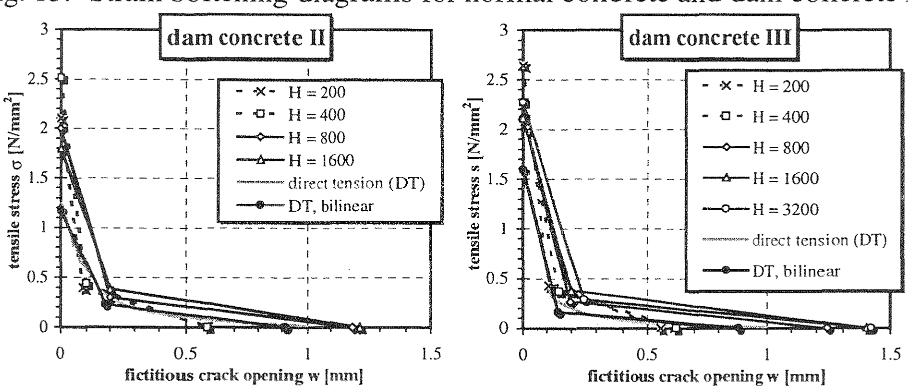

Fig. 14. Strain softening diagrams for the two types of dam concrete DC II and DC III

The strain softening as observed in the direct tension tests have been determined directly from the measured load displacement curves. The bilinear approximation has been obtained with an non-linear least square fit.

As it can be seen from the strain softening diagrams in Fig. 10 to 14 the specimens with a volume smaller than 3-times the maximum aggregate size (dashed lines) show a different strain softening behaviour as compared to the larger ones. It can also be seen, that the tensile strength f_t decreases slightly in accordance with Weibull-Theory (1939) with increasing ligament length H_L and the maximum fictitious crack opening displacement w_c increases, as it has been observed earlier by Wittmann (1990) and Wittmann et al. (1996).

5 Conclusions

From the experimental results presented in this paper we can conclude that:

- The fracture energy increases with increasing maximum aggregate and specimen size.
- For the investigated size range no limit value for the fracture energy as function of maximum aggregate size could be observed.
- For large enough specimens the fracture energy seems to reach a characteristic limit value for a given grain size.
- For specimens with a size below the representative volume fracture mechanics parameters differ strongly from the parameters obtained on larger specimens.
- If possible, fracture energy should be determined on specimens large enough in order to obtain realistic values for typical concrete structures, or the values obtained on smaller specimens must be corrected for the influence of size.

6 Acknowledgement

The authors gratefully acknowledge financial support of this project by the Swiss Federal Office of Water Resources. Stimulating discussions with Dr. Darbre from this Federal Office are worth being mentioned in particular.

7 References

Bažant, Z.P. and Cedolin, L. (1993) Why direct tension specimens break flexing to the side. **Journal of Structural Engineering**, 119 (4), 1101-1113.

Brühwiler, E. (1988) Bruchmechanik von Staumauerbeton unter quasi-statischer und erdbebendynamischer Belastung, PhD. Thesis, EPFL, Lausanne, Switzerland.

Gils van, M.A.J., Dortmans, L.J.M.G. and With de, G. (1995) Fictitious crack modelling of Kiln furniture ceramics, in **Fracture Mechanics of Concrete Structures** (ed. F.H. Wittmann), Aedificatio Publishers, Freiburg, Germany, 1261-1270.

Guofan, Z., Hui, J. and Shilang, X. (1991) Study of fracture toughness and fracture energy by means of wedge splitting test specimens, in **Brittle Matrix Composites** (eds. A.M. Brand and I.H. Marshall), Elsevier Applied Science, London & New York, 62-71.

Hillerborg, A., Modéer, M. and Petersson, P.E. (1976) Analysis of crack formation and crack growth in concrete by means of fracture mechanics and finite elements. **Cem. & Concr. Res.**, 6, 773-782.

Petersson, P.E. (1981) Crack growth and development of fracture zones in plain concrete and similar materials, Report TVBM-1006, Lund Institute of Technology, Lund, Sweden.

RILEM Recommendation AAC13.1 (1994) Determination of the specific fracture energy and strain softening of AAC, **RILEM Technical Recommendations for the testing and use of construction materials**, E & FN Spon, 156-158.

Roelfstra, P.E., Sadouki, H. and Wittmann, F.H. (1985), Le béton numérique, **Mat. And Struc.**, 18, 327–335.

Roelfstra, P.E. and Wittmann, F.H. (1986) Numerical method to link strain softening with failure of concrete, **Fracture Toughness and Fracture Energy of Concrete** (ed. Wittmann), Amsterdam, (1986) 163-175.

Slowik V., Wittmann, F.H. (1992) Influence of strain gradient on fracture energy, in **Fracture Mechanics of Concrete Structures** (ed. Z.P. Bažant), Elsevier, Amsterdam, 424-429.

Trunk, B. and Wittmann, F.H. (1998) Influence of element size on fracture mechanics parameters of concrete, **Dam Engineering**, to be published.

Weibull, W. (1939) A statistical theory of strength of materials. **Swedish Royal Institute for Engineering**, 151, Stockholm, 591-619.

Wittmann, F.H, (1990) Size effect of fracture energy of concrete. **Eng. Fract. Mech.**, 35, 107-115.

Wittmann, F.H. (1992) Fracture process zone and fracture energy, in **Fracture Mechanics of Concrete Structures** (ed. Z.P. Bažant), Elsevier, Amsterdam, 391-403.

Wittmann, X., Zhong, H. (1996) On some experiments to study the influence of size on strength and fracture energy of concrete, **Building Materials Reports**, 2, Aedificatio Publishers.